Possible neutron and proton halo structure in the isobaric analog states of $A = 12$ nuclei

A. S. Demyanova,[1] V. I. Starastsin,[1] A. N. Danilov,[1] A. A. Ogloblin,[1] S. V. Dmitriev,[1] S. A. Goncharov,[2] T. L. Belyaeva,[3] V. A. Maslov,[4] Yu. G. Sobolev,[4] W. Trzaska,[5] P. Heikkinen,[5] G. P. Gurov,[6] N. Burtebaev,[7] and D. Janseitov[7]

[1]*NRC Kurchatov Institute, Moscow RU-123182, Russia*
[2]*Lomonosov Moscow State University, GSP-1, Leninskie Gory, Moscow 119991, Russia*
[3]*Universidad Autónoma del Estado de México, C.P. 50000, Toluca, México*
[4]*Flerov Laboratory for Nuclear Research, JINR, 141980 Dubna, Moscow Region, Russia*
[5]*Department of Physics, University of Jyväskylä, FIN-40014 Jyväskylä, P.O. Box 35, Finland*
[6]*National Research Nuclear University MEPhI, Kashirskoe Shosse 31, 115409 Moscow, Russia*
[7]*Institute of Nuclear Physics, National Nuclear Center of Republic of Kazakhstan, Almaty 050032, Republic of Kazakhstan*

(Received 14 September 2020; revised 1 November 2020; accepted 6 November 2020; published 30 November 2020)

The differential cross sections of the ^{11}B(^{3}He, d) ^{12}C reaction leading to formation of the 0^+ ground state and the 15.11-MeV 1^+, 16.57-MeV 2^-, and 17.23-MeV 1^- excited states of ^{12}C are measured at $E_{\rm lab} = 25$ MeV. The analysis of the data is carried out within the coupled-reaction-channels method for the direct proton transfer to the bound and unbound states. The rms radii of the last proton in all states studied are determined. A comparison of the rms radii of the ^{12}B, ^{12}C, and ^{12}N nuclei in the isobaric analog states (IASs) with isospin $T = 1$ determined by different methods allows us to arrive at a conclusion that these nuclei in the 1^- excited states at $E_x = 2.62$, 17.23, and 1.80 MeV, respectively, possess one-nucleon (neutron or proton) halo structure. The enlarged radii and a large probability of the last neutron to be outside of the range of the interaction potential are also found for the 2^- states of ^{12}B, ^{12}C, and ^{12}N at $E_x = 1.67$, 16.57, and 1.19 MeV, respectively. These IASs also can be regarded as candidates for states with one-nucleon (neutron or proton) halo.

DOI: 10.1103/PhysRevC.102.054612

I. INTRODUCTION

In the past few decades significant progress has been made in studying the phenomenon of neutron and proton halos in excited states of stable light nuclei [1–23]. Most of these states are located close to or above the particle emission threshold. One of the necessary characteristics of a nucleus in a halo state is an increased nuclear radius or the enlarged separation distance between the core and the last nucleon. Thus, the measurement and determination of the rms radius plays a crucial role in the problem of nuclear halos. We emphasize that these exotic states of light nuclei are not limited by the neutron-halo structures. Recently the observation of a proton halo in the unbound 2.37-MeV $1/2^+$ state of ^{13}N, a mirror state with respect to the 3.09-MeV state of ^{13}C, was reported [21] . The enhanced rms radius of ^{13}N in this state was found to be equal to 2.91 ± 0.14 fm, a much larger value if compared with the radius of the ground state (g.s.) of ^{13}N of 2.31 fm. The value reported in Ref. [21] is similar to the radius of the mirror ^{13}C nucleus in the 3.09-MeV $1/2^+$ state (the estimates range from 2.7 to 2.9 fm, as shown, for instance, in Ref. [16]).

Nucleon transfer reactions are traditionally used to obtain information on single-particle (sp) states, spectroscopic factors (SF), asymptotic normalizations coefficients (ANC), and the nucleus-nucleus optical potential [6–31]. Also, these reactions are widely used to search for the states with increased radii [6,7,9,11,16,22]. Charge-exchange reactions, in particular the (^{3}He, t) reaction, are also useful for obtaining this information and have the advantage for studying unbound states in the continuum spectrum [21,23]. Note that the interpretation of a nucleon halo in the excited states located above the particle emission threshold remains an open question. In view of the lack of a way to quantitatively calculate the weight of the asymptotic part of the nucleon wave function describing the unbound state, difficulties arise in comparing its asymptotic and inner parts.

In this connection, much current interest is focused on the study of the nucleon transfer and charge-exchange reactions, in which the isobaric analog states (IASs), presumably having a halo structure, are populated. Indeed, replacing a neutron in a halo state with a proton does not necessarily lead to the appearance of an analogous proton-halo structure, and in the case of IASs having a halo, the situation is more complicated. The appearance of a halo is determined, in particular, by the proximity of the valence nucleon to the emission threshold and can be very different for a neutron and a proton. An interesting example concerns the exotic mirror ^{17}N and ^{17}Ne nuclei in their ground states. This pair has attracted a lot of interest in the last two decades in terms of their halo structure being a system formed by a core plus two nucleons. ^{17}Ne is a Borromean nucleus, which is, as accepted [24,25], has a two-proton halo. In the recent study of the neutron-rich $^{17-22}$N

isotopes [26], the increased matter radius of ^{17}N was not detected, and the halo structure for this nucleus was not confirmed. However, a thick neutron skin for the $^{19-21}$N isotopes was detected, while a developed neutron halolike structure was found for ^{22}N. This fact is not surprising if one takes into account that in ^{17}N two protons are tightly bound to the ^{15}N core with the binding energy of 8.4 MeV and in the $^{19-21}$N isotopes two protons are weakly bound or unbound to the core.

In our work, we study a triplet of the IASs with isospin $T = 1$ of the ^{12}B, ^{12}C, and ^{12}N nuclei. All these states are located in the vicinity of the nucleon emission thresholds. Taking into account the neutron halo structure in some excited states of ^{12}B, let us consider the possibility of the appearance of proton halos for other members of this multiplet. Our goal is to compare the rms radii of these nuclei in the IASs in order to reveal the possible appearance of a proton halo.

The ^{12}B nucleus is an odd-odd nucleus, and the neutron-halo structure was found in the 1.67-MeV 2^- and 2.62-MeV 1^- states of ^{12}B by studying the neutron transfer ^{11}B(d, p) ^{12}B reaction [6,7,11,22]. Namely, the following properties of these states were revealed: (1) close location to the neutron emission threshold; (2) occupation of the s and d orbitals by the valence neutron; (3) increased nuclear rms radius and halo radius; and (4) an elongated neutron wave function, which provides the probability of the last neutron to be outside of the range of the interaction radius, the so-called D_1 coefficient, larger than 50%. The combination of these properties allows one to state the appearance of a neutron halo in these excited states of ^{12}B.

The measured ^{12}B and ^{12}N spectra are very similar and their low-lying levels correspond to the one-particle–one-hole shell-model configurations [32–34]. Hence, one can expect the existence of excited states with enlarged radii and a possible proton halo in ^{12}N. The proton-emission threshold in ^{12}N is located only 0.60 MeV above the ground state, thus the IASs in ^{12}N with spin-parities 1^- and 2^- belong to the continuum spectrum. Recently, the ^{12}C$(^3$He$, t)$ ^{12}N reaction at $E(^3\text{He}) = 40$ MeV, in which the 1^+ (g.s), 2^+ (0.96 MeV), 2^- (1.19 MeV), and 1^- (1.80 MeV) states of ^{12}N were populated, has been studied [23]. The distorted wave Born approximation (DWBA) calculations and the modified diffraction model (MDM) [21,35–37] were applied to analyze the data. The MDM analysis revealed the enlarged radii for the 1.19-MeV 2^- and 1.80-MeV 1^- states in comparison with the rms radius of the g.s. of ^{12}N (2.47 ± 0.07 fm [38,39]).

The ^{12}C nucleus is one of the most studied nuclear objects and has a great importance in clustering in light nuclei and nuclear astrophysics [32,34,40–42]. Nevertheless, studying the detailed structure of the ^{12}C spectrum above 15 MeV excitation energy, especially in the region of the $T = 1$ IASs, remains an interesting and beneficial task.

We present new data for the ^{11}B$(^3$He$, d)$ ^{12}C reaction at the incident ^{3}He energy of 25 MeV. The differential cross sections are measured for the g.s. and a number of excited states of ^{12}C above $E_x = 15$ MeV. The energy levels above 5 MeV were studied by this reaction in Refs. [43–45], but we believe that the differential cross sections of the ^{11}B$(^3$He$, d)$ ^{12}C reaction to the high-lying states of ^{12}C with excitation energies of 16.57 and 17.23 MeV are reported for the first time.

We focus on the analysis of excited states with $T = 1$, which are the IASs of the corresponding states of the ^{12}B and ^{12}N nuclei. The data are analyzed by the coupled-reaction-channels (CRC) method for direct proton transfer to the bound and resonance states. The main goal of our work is to determine the radius of ^{12}C in the studied states by calculating the rms radii of the p-^{11}B sp wave functions. Finally, we summarize the recent data on the excited states with increased radii and possible neutron and proton halos in nuclei of this isospin triplet obtained by different methods.

The paper is organized as follows: Sec. II describes the experimental setup and the results of the measurements. The theoretical analysis within the CRC method for direct proton transfer is presented in Sec. III, where we also deduce the last proton rms radii of ^{12}C in the excited states. We discuss the results and compare the rms and halo radii of some light nuclei possessing neutron halos in the excited states in Sec. IV. The conclusions are presented in Sec. V.

II. EXPERIMENTAL PROCEDURE AND RESULTS

The measurements were carried out at the University of Jyväskylä (Finland) using the K130 cyclotron to produce a ^{3}He beam at $E_{\text{lab}} = 25$ MeV. The 150-cm-diameter Large Scattering Chamber (LSC) [46] equipped with three sets of ΔE-E detector telescopes, each containing two independent ΔE detectors and one common E detector, was used. Each device allowed carrying out measurements at two angles. The measurements in center-of-mass (c.m.) angular range 10° were conducted in one exposure. Two silicon pin diodes of 380 and 100 μm were operating as ΔE detectors and 3.6 mm lithium-drifted silicon detectors were used as E detectors. The differential cross sections of the ^{11}B$(^3$He$, d)$ ^{12}C reaction were measured in the c.m. angular range 4°–60°. The beam intensity was about 20 particle nA. A self-supported enriched (95%) boron foil of 0.275 mg/cm^2 thickness was used as a ^{11}B target. The ^{10}B, ^{12}C, and ^{14}N nuclei were impurities in the target, so peaks for the excited states of ^{11}C, ^{13}N, and ^{15}O are also present in the measured spectra. Fortunately, this did not compromise our measurements as all the levels below the excitation energy of 15 MeV were well separated thanks to the total energy resolution of about 80–120 keV. This very good energy resolution was needed to resolve the 4^- or 2^- and 1^+ states in ^{12}C, which was achieved with a monochromatization method described in Ref. [46]. The procedure reduces the energy spread of the native cyclotron beam by a factor of 2 to 3, hence making this measurement possible.

In Fig. 1 a sample deuteron spectrum from the ^{11}B$(^3$He$, d)$ ^{12}C reaction at $\theta_{\text{lab}} = 23°$ showing the excited states of ^{12}C up to $E_x \approx 23.5$ MeV with both the isospins $T = 0$ and $T = 1$ is presented. The spectrum peaks were identified and parametrized using a standard decomposition method: the spectrum peaks were fitted with a Gaussian shape. With the known energy calibration, the peak positions and widths were fixed in accordance with the generally accepted values, while the areas under the peaks were treated as free parameters. In Fig. 1(b), a decomposition of the spectrum region from 16 to 19 MeV is shown in detail.

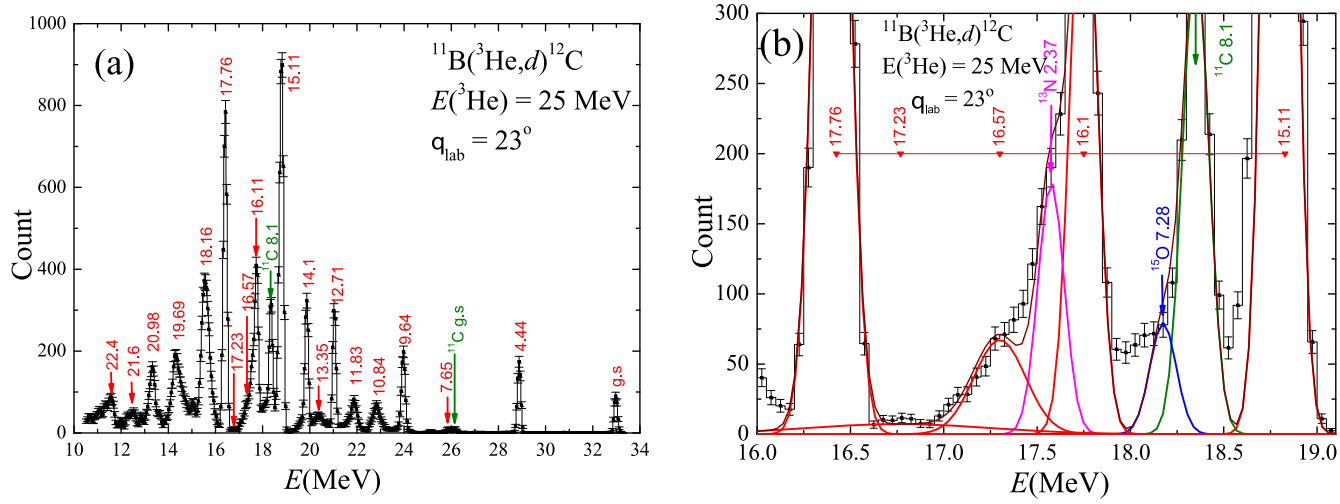

FIG. 1. (a) A deuteron spectrum from the ^{11}B(^{3}He, d) ^{12}C reaction at $\theta_{\text{lab}} = 23^\circ$ with the excitation of ^{12}C states up to $E_x \approx 22.5$ MeV. (b) The detailed spectrum region from 16 to 19 MeV.

As a result the deuteron angular distribution for the g.s. and the excited 15.11-, 16.57-, 17.23-MeV states of ^{12}C were extracted using the ^{11}B(^{3}He, d) ^{12}C. The resulting differential cross sections are presented in Figs. 2–5.

III. THEORETICAL ANALYSIS

We study the excited states of ^{12}C with $T = 1$: 15.11-MeV 1^+, 16.57-MeV 2^-, and 17.23-MeV 1^- states, which are excited through a proton-transfer ^{11}B(^{3}He, d) ^{12}C reaction. Accordingly to the charge independence of nuclear forces, these states are the IASs of the 1^+ g.s., the 1.67-MeV 2^-, and the 2.62-MeV 1^- states of ^{12}B. They are also the IASs of the 1^+ g.s, 1.19-MeV 2^-, and 1.80-MeV 1^- states of ^{12}N [32,34].

A. Elastic scattering analysis

The first step of the analysis includes choosing reasonable optical potentials (OPs) to fit the experimental elastic-scattering angular distribution. The effective potentials are represented by the OPs of the standard form:

$$\mathbf{V}(r) = V_{\text{Coul}}(r) - V_0 f_0(r) + V_{\text{s.o.}}\left(\frac{\hbar}{m_\pi c}\right)^2 2(\mathbf{L}\cdot\mathbf{s}) \times \frac{1}{r}\frac{d}{dr} f_{\text{s.o.}}(r) - i\left[W - 4W_D \frac{d}{dr}\right] f_W(r), \quad (1)$$

$$f_i(r) = \left\{1+\exp\left[\left(r - r_i A_T^{1/3}\right)/a_i\right]\right\}^{-1}, \quad i = 0,\ \text{s.o., and } W, \quad (2)$$

with the real, spin-orbital, and imaginary components, respectively. The Coulomb interaction is represented by the $V_{\text{Coul}}(r)$ potential of a uniformly charged sphere of radius $R_C = r_C A_T^{1/3}$.

Parameters of the OP used for the $^3\text{He} + ^{11}\text{B}$ channel at 25 MeV are chosen based on the global parametrization presented in Refs. [47] and taking into account the elastic scattering and reaction coupling effect. The final sets of parameters (see Table I) correspond to the best fit of the elastic-scattering data available at laboratory energy around 25 MeV.

Parameters of the OPs describing the $d + ^{12}$C interaction at 17–20 MeV are calculated based on the global parametrization presented in Ref. [48] and taking into account the corresponding energy dependence of the depths and radial parameters of OPs (see Table I).

B. Coupled-reaction-channels analysis

Our analysis is performed within the CRC method by using the code FRESCO [49]. Calculations of the differential cross sections of the ^{11}B(^{3}He, d) ^{12}C reaction are carried out in the framework of the one-proton direct transfer mechanism to the bound and unbound excited states of ^{12}C: $^3\text{He}(I_{\text{He}}) + ^{11}\text{B}(I_{\text{B}}) \rightarrow [d(I_d) + p(s_p)] + ^{11}\text{B}(I_{\text{B}}) \rightarrow d(I_d) + ^{12}\text{C}(I_{\text{C}})$. This mechanism is characterized by the following angular-momentum coupling scheme (see, e.g., [50]):

$$\begin{aligned} \mathbf{I}_{\text{He}} &= \mathbf{j}_1 + \mathbf{I}_d\,, \qquad \mathbf{j}_1 = \mathbf{s}_p + \mathbf{l}_1, \\ \mathbf{I}_{\text{C}} &= \mathbf{j}_2 + \mathbf{I}_{\text{B}}, \qquad \mathbf{j}_2 = \mathbf{s}_p + \mathbf{l}_2, \\ \mathbf{L} &= \mathbf{j}_1 + \mathbf{j}_2 = \mathbf{l}_1 + \mathbf{l}_2, \end{aligned} \quad (3)$$

where s_p, I_d, I_{He}, I_{C}, and I_{B} are proton, deuteron, ^{3}He, ^{12}C, and ^{11}B spins, L is the transferred orbital angular momentum, and l_1 (l_2) and j_1 (j_2) are the orbital and total angular momenta of the proton in ^{3}He (^{12}C).

In the accepted two-body approximation, the model sp wave functions are used instead of the exact overlap wave functions, which describe the proton wave function in the corresponding state of ^{3}He and ^{12}C. If the proton is bound at negative energy ε_p around the core, then its wave function is found as the eigensolution of a given potential with boundary conditions corresponding to the bound state by varying the depth of the binding potential.

We use the proton $1s_{1/2}$ sp wave function in ^{3}He with orbital angular momentum $l_1 = 0$ generated by the Woods-Saxon potential with the depth of 76.3 MeV, the radius $R =$ 1.13 fm, and the diffuseness parameter $a = 0.95$

TABLE I. Parameters of the optical model potentials for the ^{11}B(^{3}He, d) ^{12}C reaction calculations.

Channel	V_0 (MeV)	r_0 (fm)	a_0 (fm)	W (MeV)	r_W (fm)	a_W (fm)	W_D (MeV fm)	r_{W_D} (fm)	a_{W_D} (fm)	$V_{\text{s.o.}}$ (MeV)	$r_{\text{s.o.}}$ (fm)	$a_{\text{s.o.}}$ (fm)	r_C (fm)
^{3}He + ^{11}B	123.0	1.184	0.732	4.0	1.42	0.823	11.0	1.207	0.775	2.07	0.747	0.88	1.289
d + ^{12}C	94.40	1.050	0.776	4.8	1.87	0.730	3.0	1.87	0.730	1.0	0.8	0.5	1.3

fm. This wave function is characterized by the sp ANC $b_{pd,l_1=0,j_1=1/2} = 2.076$ fm$^{-1/2}$ in accordance with Ref. [51].

The structure of the ^{12}C levels is considered in terms of the shell model and corresponds to a population of the single-proton states (their configurations are presented in Table II). It is assumed that the last proton occupies the $1p_{3/2}$ orbital in the 0^+ g.s. of ^{12}C and the $1p$, $2s$, $1d$, $1f$, and $1g$ shells in the other studied excited states of ^{12}C. The radial quantum number n_r defines directly the number of nodes in the radial solution.

Cross section calculations to the bound states of ^{12}C are carried out with the normalized sp overlap $p + ^{11}$B wave functions generated by the $V_{^{11}\text{B}p}(r)$ potential of Woods-Saxon shape with varying radii and diffuseness parameters. The depth of the $V_{^{11}\text{B}p}$ potential is adjusted to fit the proton binding energy in given state. The geometric parameters and the spectroscopic amplitudes $\Theta^{\text{expt}}_{n_2 l_2 j_2}$ (the reduced widths) are adjusted to fit the differential cross sections, especially in the region of the main peak.

The asymptotic behavior for $r > R_{\text{N}}$ (R_{N} is the channel radius) of the radial sp overlap wave function is described by the Whittaker function dependent on the binding energy ε_p and is proportional to the sp ANC b_{nl}. Given that the bound nucleon radial wave function is square integrable (normalized to unity), its rms radius is associated with the rms distance between the last nucleon and the core [6,7,9,11,16,22].

Optimal sets of the geometric parameters of the ^{11}B + p interaction potentials giving the best fit to the data for different states are shown in Table II, as well as the sp ANC $b_{n_2 l_2}$. The calculated differential cross sections of the ^{11}B(^{3}He, d) ^{12}C reaction to the g.s. and the bound 15.11-MeV 1^+ state are shown (by lines) in Figs. 2 and 3 in comparison with the measured data.

The threshold of proton emission in ^{12}C lies at $E_{\text{th}} = 15.96$ MeV, so the 16.57-MeV 2^- and the 17.23-MeV 1^- states are the resonant continuum states with widths of 0.3 and 1.15 MeV, respectively [32,34].

Cross-section calculations to the unbound states of ^{12}C with spin I_{C} are carried out with the scattering wave functions corresponding to the resonant scattering of a proton on the core ^{11}B nucleus. The asymptotic parts of the resonant wave functions are described in terms of their S-matrix elements. In order to calculate a form factor of a continuum state, the resonant energy-averaged wave function, the so-called "bin" wave function [52]

$$\Phi(r) = \sqrt{\frac{2}{\pi N}} \int_{k_1}^{k_2} w(k)\varphi_k(r)dk \tag{4}$$

TABLE II. The excitation energy, spin-parity, proton binding energy, level width, depth, and geometric parameters of the ^{11}B + p interaction potential, sp quantum numbers (the radial quantum number, orbital and total angular momenta), sp ANC, spectroscopic amplitude, and the last proton rms radius for the states of ^{12}C.

E_x (MeV)	J^π_f	ε_p (MeV)	Γ (keV)	V_0 (MeV)	r_0 (fm)	a (fm)	$n_{r,2}$	l_2	j_2	$b_{n_2 l_2}$ (fm$^{-1/2}$)	$\Theta^{\text{expt}}_{n_2 l_2 j_2}$	R_p (fm)
0.0	0^+	−15.96			1.5	0.80	1	1	3/2	15.82	1.0	2.9 ± 0.1
15.11	1^+	−0.85			1.30	0.65	1	1	1/2	1.28	0.18	4.0 ± 0.2
							1	1	3/2	1.23	0.18	
							1	1	5/2	0.07	0.13	
16.57	2^-	0.61	300	150	1.20	0.855	2	0	1/2		1.55	
							1	2	3/2		0.64	
							1	2	5/2		0.64	
							1	4	7/2		0.40	
16.57	2^-	−0.01			1.25	0.65	2	0	1/2		0.40	6.76 ± 0.35
							1	2	3/2		0.16	
							1	2	5/2		0.16	
							1	4	7/2		0.10	
17.23	1^-	1.27	1150	150	1.25	0.90	2	0	1/2		0.34	
							1	2	3/2		0.23	
							1	2	5/2		0.23	
17.23	1^-	−0.01			1.25	0.75	2	0	1/2		0.29	7.05 ± 0.35
							1	2	3/2		0.18	
							1	2	5/2		0.18	

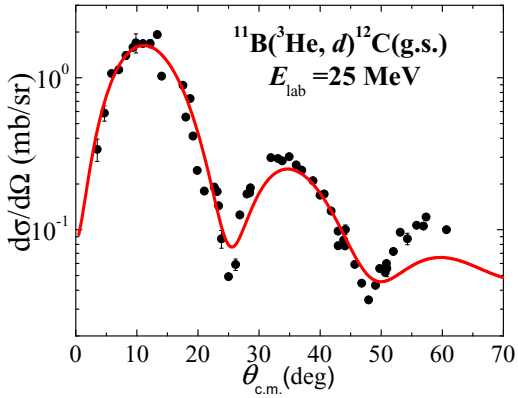

FIG. 2. Deuteron angular distribution from the ^{11}B(^{3}He, d) ^{12}C reaction populated the 0^+ ground state of ^{12}C at $E_{lab} = 25$ MeV (squares) in comparison with the CRC (line) calculation.

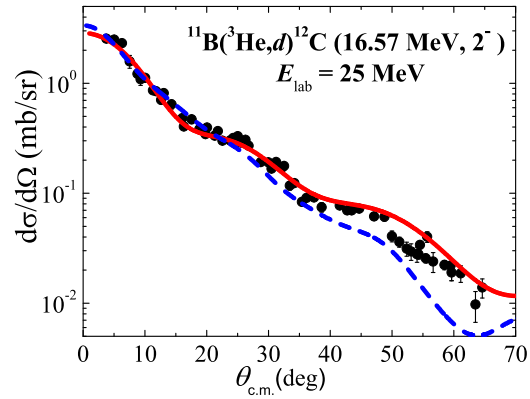

FIG. 4. Deuteron angular distribution from the ^{11}B(^{3}He, d) ^{12}C reaction populated the excited 16.57-MeV 2^- state. The solid and dashed lines correspond to the CRC calculations with the bound and resonant wave functions.

is introduced. Averaging is carried out over the energy bin range $k_1 \leqslant k \leqslant k_2$, where $k = [\sqrt{2\mu(E_x - E_{th})}]/\hbar$ is the linear momentum of a proton relative to ^{11}B in ^{12}C, μ is the reduced mass, and E_x is the excitation energy of the unbound state. The $\varphi_k(r)$ are the continuum solutions of the scattering Woods-Saxon potential (the depth and the geometric parameters are shown in Table II). The wave functions $\Phi(r)$ are normalized to unity, $\langle \Phi \mid \Phi \rangle = 1$, within a sufficiently large integration interval over r (we choose a maximum radius $R = 400$ fm). To ensure convergence of $\Phi(r)$, the normalized weight functions $w(k)$ corresponding to the resonance behavior,

$$w(k) = \exp(-i\delta_k)\sin(\delta_k), \tag{5}$$

$$N = \int_{k_1}^{k_2} |w(k)|^2 dk, \tag{6}$$

are introduced, where δ_k are the scattering phase shifts for $\varphi_k(r)$.

We calculate the reaction cross sections by using two different proton wave functions in the excited state of ^{12}C: (a) the resonant wave functions $\Phi(r)$ [Eq. (4)] and (b) the bound wave functions calculated with the small (fictitious) negative (−0.01 MeV) binding energy of the valence proton. Figures 4 and 5 show the differential cross sections calculated with the bound (solid lines) and the resonant (dashed lines) wave functions.

Calculations with both wave functions reproduce the experimental deuteron angular distributions in a similar way; therefore the calculations with bound wave functions could be taken as a good approximation. It is obvious that the absolute values of the experimental spectroscopic amplitudes $\Theta^{expt}_{n_2 l_2 j_2}$ determined from the calculations with continuum and bound wave functions are different, but the relative weights of the sp configurations are found to be the same (within the error bars) regardless of the choice of the wave functions. The values of $\Theta^{expt}_{n_2 l_2 j_2}$ deduced from our CRC analysis are shown in Table II for both cases.

It is well known that the shape of the proton + core (p + ^{11}B and $p + d$) interaction potential defined by the geometric parameters strongly affects the differential cross section of the proton transfer reaction. In nucleon transfer reactions, this influence mainly affects the spectroscopic amplitudes and, to the same extent, the shape of the angular distributions. The

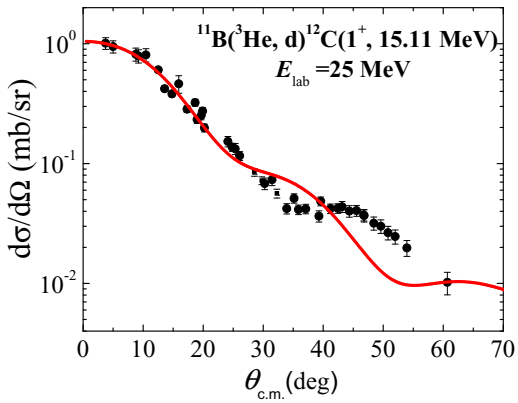

FIG. 3. The same as in Fig. 2, but for the excited 15.11-MeV 1^+ state.

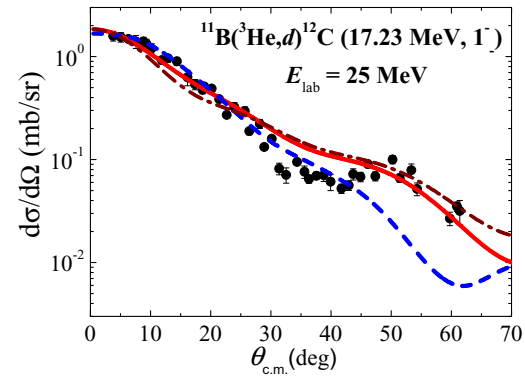

FIG. 5. The same as in Fig. 4, but for the excited 17.23-MeV 1^- state. The dash-dotted line corresponds to the CRC calculations with the geometric parameters $r_0 = 1.20$ fm and $a_0 = 0.50$ fm.

TABLE III. The spin-parities, excitation energies, rms matter radii, and D_1 coefficients of the ^{12}B, ^{12}C, and ^{12}N nuclei in the isobaric analog $T = 1$ states.

	^{12}B			^{12}C			^{12}N	
J^π_f	E_x (MeV)	$R_{\rm rms}$ (fm)	D_1 %	E_x (MeV)	$R_{\rm rms}$ (fm)	D_1 %	E_x (MeV)	$R_{\rm rms}$ (fm)
1^+	0.0	2.39 ± 0.02[a]	11[b]	15.11	2.40 ± 0.06	30	0.0	2.47 ± 0.07[c]
2^-	1.67	2.73 ± 0.11[b]	53[b]	16.57	2.88 ± 0.13	47	1.19	2.8 ± 0.2[d]
1^-	2.62	3.00 ± 0.11[b]	62[b]	17.23	2.94 ± 0.13	52	1.80	3.3 ± 0.2[d]

[a]Reference [54].
[b]Reference [22] by using $R_{\rm rms}(^{11}{\rm B}) = 2.29$ fm.
[c]Reference [55].
[d]Reference [23].

best description of the data and reasonable or known values of the SFs are the criteria for selecting potential parameters. We studied the effect of the parameter choice in detail in the previous works [16,22]. In the current calculations, the best fit of the experimental deuteron angular distributions for the high-lying states is achieved using the geometric parameters of the ^{11}B $+p$ interaction potential with nearly standard values (see Table II). The last column of Table II contains the values of the rms radius of the bound sp wave functions (the last proton rms radius), R_p, in the studied states of ^{12}C. It is evident that R_p decreases with decreasing geometric parameters of the interaction potential. In Fig. 5, by way of illustration, we show (by dash-dotted line) the cross section of this reaction populating the 17.32-MeV 1^- state, which is calculated with the reduced geometric parameters $r_0 = 1.2$ fm and $a_0 = 0.50$ fm. One can see that the agreement of this calculation with the data is significantly worse. Thus, the derived error bars for R_p of approximately 5% characterize the ambiguity in determining the geometric parameters and the fictitious binding energy (from -0.005 to -0.1 MeV).

IV. DISCUSSION

Let us estimate the radii of ^{12}C in the continuum excited states using the last proton rms radius R_p, which is approximated as the rms radius of the bound sp proton wave function in ^{12}C. It should be noted that R_p for the 16.57-MeV 2^- and the 17.23-MeV 1^- states are significantly enhanced in comparison with those for the g.s. and the 15.11 -MeV 1^+ state (see Table II). The most important result follows form the comparison of the rms radii of the ^{12}C, ^{12}B, and ^{12}N nuclei in the corresponding $T = 1$ IASs. It is evident that if the halo state is characterized by the extended radius of the valence particle, the nucleus in this state has an increased matter radius. This fact is definitely seen from Table III, where the rms matter radii of the ^{12}B, ^{12}C, and ^{12}N nuclei in the studied IASs are shown. In order to calculate the nuclear rms radii, a relationship [53] between the one-proton (one-neutron) radius R_p and the rms radii $R_{\rm rms}$ of the core-nucleus A and the $(A + 1)$ system,

$$(A+1)[R_{\rm rms}(A+1)]^2 = A[R_{\rm rms}(A)]^2 + [A/(A+1)]R_p^2, \quad (7)$$

is used.

Table III shows the summary of the rms radii, $R_{\rm rms}$, of the ^{12}B, ^{12}C, and ^{12}N nuclei in the IASs with $T = 1$ calculated in this work and obtained by other different methods in Refs. [22,23,54–56]. The rms radii of ^{12}C and ^{12}B are calculated accordingly to Eq. (7) taking into account the rms matter radius of ^{11}B, $R_{\rm rms}(^{11}{\rm B}) = 2.29$ fm. This value corresponds to the average value of the rms radius of ^{11}B presented in different references mentioned in Ref. [57] (note that in Ref. [22], $R_{\rm rms}(^{11}{\rm B}) = 2.09$ fm was used following Ref. [38]).

In accordance with a rigorous definition of a halo state for exotic nuclei, it is assumed that the halo nucleon would spend about 50% of the time outside the range of the core potential [58–62]. This is a sufficiently strict requirement, whereas there are many "real halos" that are large, but have up to 50% of the nucleon wave function remaining within the potential well [58]. Also, less developed halos and halolike states do not exactly satisfy this criterion. To calculate this probability quantitatively, a coefficient $D_1(R_{\rm N})$ estimating the weight of the asymptotic part of the wave function is introduced,

$$D_1(R_{\rm N}) = \int_{R_{\rm N}}^{\infty} u_{lj}^2(r) r^2 dr, \quad (8)$$

where $u_{lj}(r)$ is a sp nucleon radial wave function. In Table III, calculated values of $D_1(R_{\rm N})$ in percent at the distance about $R_{\rm N} = 5.0$ fm are also shown.

Our calculations show that the rms radii of the last proton in all excited states under consideration are greater than that in the g.s. of ^{12}C.

The largest radii are found for the 1^- states at $E_x = 2.62$, 17.23, and 1.80 MeV of ^{12}B, ^{12}C, and ^{12}N, respectively. It was claimed in Refs. [6,7,11,22] that ^{12}B in this state possesses a neutron halo in view of not only the enlarged rms neutron radius and the rms matter radius, but also the D_1 coefficient value much greater than 50%. A similar result is obtained for ^{12}C in the corresponding IAS: the enlarged rms proton radius (7.1 ± 0.3 fm), the increased rms matter radius (2.94 ± 0.13), and $D_1 = 52\%$. The detected tendency can be traced in the corresponding IAS of the ^{12}N nucleus, where a very enlarged rms radius (3.3 ± 0.2 fm) was found by the MDM in Ref. [23]. Thus, we can propose that the excited 1^- states at 17.23 MeV in ^{12}C and 1.80 MeV in ^{12}N possess the proton halo structure.

In Refs. [6,22], it was found that the 1.67-MeV 2^- state of ^{12}B also can be considered as a halo state, with the last neutron spending more than 50% of its time outside the range of the core potential and the neutron rms radius $R_n(2^-) = R_h(2^-) = 5.9 \pm 0.3$ fm, which exceeds that for the g.s. by a factor of 1.7. We determine the rms radius of the last proton in the corresponding IAS of ^{12}C at 16.57 MeV excitation energy to be equal to 6.76 ± 0.30 MeV. The rms matter radius of ^{12}C in this state calculated by Eq. (7) is $R_{rms} = 2.88 \pm 0.13$ fm, which is by a factor of 1.2 greater than that for its g.s. [$R_{rms}(^{12}C_{g.s.}) = 2.35 \pm 0.02$ fm]. The weight of the asymptotic part of the proton wave function, $D_1 = 47\%$, is slightly less than 50%. The MDM analysis performed in Ref. [23] also revealed the enlarged rms matter radius (2.8 ± 0.2 fm) for the corresponding IAS of the ^{12}N nucleus. With respect to these 2^- excited states at 16.57 MeV in ^{12}C and 1.19 MeV in ^{12}N, we can suggest a possible proton halolike structure.

Our results confirm the statement above that the halo phenomenon has a universal character and appears both in the ground states of exotic nuclei and in the excited states of normal light nuclei. This statement is based on the enlarged radii obtained in our works by different methods, as well as the respective large values of the D_1 coefficient, which prove a large probability of finding the last nucleon, neutron or proton, outside the range of the sp interaction potential.

V. CONCLUSIONS

In recent years, studies of the nucleon transfer and charge-exchange reactions populating isobaric analog states of light nuclei have attracted considerable interest in view of their relation with the neutron and proton halo structure of light nuclei. In this work we studied a triplet of IASs with isospin $T = 1$ in the ^{12}B, ^{12}C, and ^{12}N nuclei and compared their rms radii. The appearance of neutron halo states of ^{12}B was demonstrated in Refs. [6,7,11,22], where the neutron transfer $^{11}B(d, p)^{12}B$ reaction was analyzed by the ANC method. The $^{12}C(^3He, t)^{12}N$ charge-exchange reaction was studied in Ref. [23] and the proton halo in the corresponding IASs of ^{12}N was revealed by the MDM analysis. In our work, we measured the differential cross sections of the proton transfer $^{11}B(^3He, d)^{12}C$ reaction to the g.s. and the excited 15.11, 16.57, 17.23 MeV states of ^{12}C at 25 MeV with the aim of finding a possible proton halo appearance in the IASs with isospin $T = 1$ of the ^{12}C nucleus.

A theoretical analysis of the data was carried out in the framework of the CRC method for direct proton transfer. We calculated the reaction cross sections to the unbound resonance states of ^{12}C in the continuum by using two different proton wave functions: the resonant wave functions and the bound wave functions calculated with the effective small negative binding energy of the valence proton. A comparison of the calculated cross sections allowed us to estimate the last proton rms radii in the 16.57-MeV 2^- and 17.23-MeV 1^- states of ^{12}C, which were found to be significantly enlarged. Finally, we compared the rms radii of ^{12}B, ^{12}C, and ^{12}N in the IASs with isospin $T = 1$ determined by different methods and arrived at a conclusion that the ^{12}B, ^{12}C, and ^{12}N nuclei in the 1^- excited states at $E_x = 2.62$, 17.23, and 1.80 MeV, respectively, possess one-nucleon (neutron or proton) halo structure. This conclusion is based on the rms radius calculations and estimates of the weight of the asymptotic part of the single-particle wave functions (D_1 coefficient values). The enlarged radii and large values of D_1 coefficient are also found for the 2^- states of ^{12}B, ^{12}C, and ^{12}N at $E_x = 1.67$, 16.57, and 1.19 MeV, respectively. These IASs can be also regarded as candidates for states with one-nucleon (neutron or proton) halo.

ACKNOWLEDGMENTS

The authors are indebted to the anonymous referee for a careful examination of the manuscript, which improved its clarity and impact. This work was supported by Russian Science Foundation Grant No. 18-12-00312 (Russia).

[1] Y. Suzuki and K. Yabana, Phys. Lett. B **272**, 173 (1991).
[2] T. Otsuka, N. Fukunishi, and H. Sagawa, Phys. Rev. Lett. **70**, 1385 (1993).
[3] T. Otsuka, M. Ishihara, N. Fukunishi, T. Nakamura, and M. Yokoyama, Phys. Rev. C **49**, R2289 (1994).
[4] K. Arai, Y. Suzuki, and K. Varga, Phys. Rev. C **51**, 2488 (1995).
[5] R. Morlock, R. Kunz, A. Mayer, M. Jaeger, A. Muller, J. W. Hammer, P. Mohr, H. Oberhummer, G. Staudt, and V. Kolle, Phys. Rev. Lett. **79**, 3837 (1997).
[6] Z. H. Liu, C. J. Lin, H. Q. Zhang, Z. C. Li, J. S. Zhang, Y. W. Wu, F. Yang, M. Ruan, J. C. Liu, S. Y. Li, and Z. H. Peng, Phys. Rev. C **64**, 034312 (2001).
[7] C. J. Lin, Z. H. Liu, H. Q. Zhang, Y. W. Wu, F. Yang, and M. Ruan, Chin. Phys. Lett. **18**, 1183 (2001).
[8] Z. Li, W. Liu, X. Bai, Y. Wang, G. Lian, Z. Li, and S. Zeng, Phys. Lett. B **527**, 50 (2002).
[9] Z. H. Liu, Chin. Phys. Lett. **19**, 1071 (2002).
[10] J. Al-Khalili and K. Arai, Phys. Rev. C **74**, 034312 (2006).
[11] B. Guo, Z. H. Li, W. P. Liu, and X. X. Bai, J. Phys. G: Nucl. Part. Phys. **34**, 103 (2007).
[12] C. Romero-Redondo, E. Garrido, D. V. Fedorov, and A. S. Jensen, Phys. Lett. B **660**, 32 (2008).
[13] A. A. Ogloblin, A. N. Danilov, T. L. Belyaeva, A. S. Demyanova, S. A. Goncharov, and W. Trzaska, Phys. Rev. C **84**, 054601 (2011).
[14] A. A. Ogloblin, A. N. Danilov, T. L. Belyaeva, A. S. Demyanova, S. A. Goncharov, and W. Trzaska, Yad. Fiz. **74**, 1581 (2011) [Phys. At. Nucl. **74**, 1548 (2011)].
[15] K. Riisager, Phys. Scr. T **152**, 014001 (2013).
[16] T. L. Belyaeva, R. Perez-Torres, A. A. Ogloblin, A. S. Demyanova, S. N. Ershov, and S. A. Goncharov, Phys. Rev. C **90**, 064610 (2014).
[17] A. S. Demyanova *et al.*, JETP Lett. **102**, 413 (2015).
[18] A. S. Demyanova, A. A. Ogloblin, A. N. Danilov, T. L. Belyaeva, S. A. Goncharov, and W. Trzaska, JETP Lett. **104**, 526 (2016).

[19] Shubhchintak, Phys. Rev. C **96**, 024615 (2017).
[20] A. A. Ogloblin, A. N. Danilov, A. S. Demyanova, S. A. Goncharov, T. L. Belyaeva, and W. Trzaska, *Nuclear Particle Correlations and Cluster Physics* (World Scientific, Singapore, 2017), p. 311.
[21] A. S. Demyanova, A. A. Ogloblin, S. A. Goncharov, A. N. Danilov, T. L. Belyaeva, and W. Trzaska, Phys. At. Nucl. **80**, 831 (2017).
[22] T. L. Belyaeva *et al.*, Phys. Rev. C **98**, 034602 (2018).
[23] A. S. Demyanova *et al.*, JETP Lett. **111**, 409 (2020).
[24] L. V. Grigorenko, Yu. L. Parfenova, and M. V. Zhukov, Phys. Rev. C **71**, 051604(R) (2005).
[25] R. Kanungo *et al.*, Eur. Phys. J. A **25**, 327 (2005).
[26] S. Bagchi *et al.*, Phys. Lett. B **790**, 251 (2019).
[27] J. Yang and P. Capel, Phys. Rev. C **98**, 054602 (2018).
[28] N. T. T. Phuc, N. H. Phuc, and D. T. Khoa, Phys. Rev. C **98**, 024613 (2018).
[29] N. T. T. Phuc, R. S. Mackintosh, N. H. Phuc, and D. T. Khoa, Phys. Rev. C **100**, 054615 (2019).
[30] L. Moschini, J. Yang, and P. Capel, Phys. Rev. C **100**, 044615 (2019).
[31] C. Hebborn and P. Capel, Phys. Rev. C **100**, 054607 (2019).
[32] F. Ajzenberg-Selove, Nucl. Phys. A **506**, 1 (1990).
[33] K. Peräjärvi, C. B. Fu, G. V. Rogachev, G. Chubarian, V. Z. Goldberg, F. Q. Guo, D. Lee, D. M. Moltz, J. Powell, B. B. Skorodumov, G. Tabacaru, X. D. Tang, R. E. Tribble, B. A. Brown, A. Volya, and J. Cerny, Phys. Rev. C **74**, 024306 (2006).
[34] J. N. Keley, J. E. Purcell, and C. S. Sheu, Nucl. Phys. A **968**, 71 (2017).
[35] A. S. Demyanova, A. A. Ogloblin, S. A. Goncharov, and T. L. Belyaeva, Int. J. Mod. Phys. E **17**, 2118 (2008).
[36] A. S. Demyanova, T. L. Belyaeva, A. N. Danilov, Yu. A. Glukhov, S. A. Goncharov, S. V. Khlebnikov, V. A. Maslov, Yu. D. Molchalov, Yu. E. Penionzhkevich, R. V. Revenko, M. V. Safonenko, Yu. G. Sobolev, W. Traska, G. P. Tyurin, and A. A. Ogloblin, Phys. At. Nucl. **72**, 1611 (2009).
[37] A. N. Danilov, T. L. Belyaeva, A. S. Demyanova, S. A. Goncharov, and A. A. Ogloblin, Phys. Rev. C **80**, 054603 (2009).
[38] A. Ozawa *et al.*, Nucl. Phys. A **691**, 599 (2001).
[39] A. Ozawa, T. Suzuki, and I. Tanihata, Nucl. Phys. A **693**, 32 (2001).
[40] M. Freer and H. O. U. Fynbo, Prog. Part. Nucl. Phys. **78**, 1 (2014).
[41] T. L. Belyaeva, A. N. Danilov, A. S. Demyanova, S. A. Goncharov, A. A. Ogloblin, and R. Perez-Torres, Phys. Rev. C **82**, 054618 (2010).
[42] S. Ohkubo, J. Takahashi, and Y. Yamanaka, Prog. Theor. Exp. Phys. **2020**, 041D01 (2020).
[43] M. A. Crosby and J. C. Legg, Nucl. Phys. A **95**, 639 (1967).
[44] P. D. Miller, J. L. Duggan, M. M. Duncan, R. L. Dangle, W. R. Coker, and L. Jung, Nucl. Phys. A **136**, 229 (1969).
[45] G. M. Reynolds, D. E. Rundquist, and R. M. Poichar, Phys. Rev. C **3**, 442 (1971).
[46] W. H. Trzaska *et al.*, Nucl. Instrum. Methods Phys. Res., Sect. A **903**, 241 (2018).
[47] C.-T. Liang, X.-H. Li, and C.-H. Cai, J. Phys. G: Nucl. Part. Phys. **36**, 085104 (2009).
[48] Y. Zhang, D. Y. Pang, and J. L. Lou, Phys. Rev. C **94**, 014619 (2016).
[49] I. J. Thompson, FRESCO user's manual, version FRES 2.9, University of Surrey, United Kingdom, 2006, available in www.fresco.org.uk/.
[50] G. R. Satchler, *Direct Nuclear Reactions* (Clarendon, Oxford, 1983).
[51] R. Yarmukhamedov and L. D. Blokhintsev, Phys. At. Nucl. **81**, 616 (2018).
[52] I. J. Thompson, Comput. Phys. Rep. **7**, 167 (1988).
[53] J. A. Tostevin and J. S. Al-Khalili, Nucl. Phys. A **616**, 418 (1997).
[54] I. Tanihata *et al.*, Phys. Lett. B **206**, 592 (1988).
[55] A. Ozawa *et al.*, Nucl. Phys. A **583**, 807c (1995).
[56] J. Li, P. Liu, J. Wang, Z. Hu, R. Mao, C. Li, R. Chen, Z. Sun, H. Xu, G. Xiao, and Z. Guo, Chin. Phys. Lett. **27**, 032501 (2010).
[57] J. H. Kelley, E. Kwana, J. E. Purcell, C. G. Sheua, and H. R. Weller, Nucl. Phys. A **880**, 88 (2012).
[58] K. Riisager, Rev. Mod. Phys. **66**, 1105 (1994).
[59] K. Riisager, D. V. Fedorov, and A. S. Jensen, Europhys. Lett. **49**, 547 (2000).
[60] A. S. Jensen and M. V. Zhukov, Nucl. Phys. A **693**, 411 (2001).
[61] A. S. Jensen, K. Riisager, D. V. Fedorov, and E. Garrido, Rev. Mod. Phys. **76**, 215 (2004).
[62] B. Jonson, Phys. Rep. **389**, 1 (2004).